POLITECNICO
MILANO 1863

SCUOLA DI INGEGNERIA INDUSTRIALE
E DELL'INFORMAZIONE

Executive Summary of the Thesis

Optical and SAR methods analysis for oil tanks height estimation

Laurea Magistrale in Telecommunication Engineering - Ingegneria delle Telecomunicazioni

Author: Eleonora Arnese

Advisor: Prof. Andrea Virgilio Monti-Guarnieri

Academic year: 2021-2022

1. Introduction

One of the most interesting and challenging studies in the field of remote sensing is the estimation of some information about man-made constructions on the Earth surface. In particular, this thesis focuses on the analysis and application of specific remote sensing methodologies to oil tanks. Monitoring this type of structures [1] is very important since their content is often dangerous, being easily flammable. In addition, extracting automatically some geometrical parameters of oil tanks by means of remote sensing techniques saves companies time, which otherwise would have to do it by hand. Moreover, these parameters could help to calculate the oil level, through the height of the floating roof which increases or decreases according to it, that is particularly significant for economics and trade. The parameter in analysis will be the height of the tank. In order to achieve this goal, methods based on optical and Synthetic Aperture Radar (SAR) have been exploited. Existing techniques employ Very High Resolution sensors; with respect to this approach, the proposed methods in this thesis are analysed both for high and low resolution, since these latter types of data are more readily available compared to high resolution and they are also free. For this class of sensors Sentinel-1 and Sentinel-2 images are exploited.

2. Proposed methods

A scheme of methods that have been proposed is summarized in figure 1.

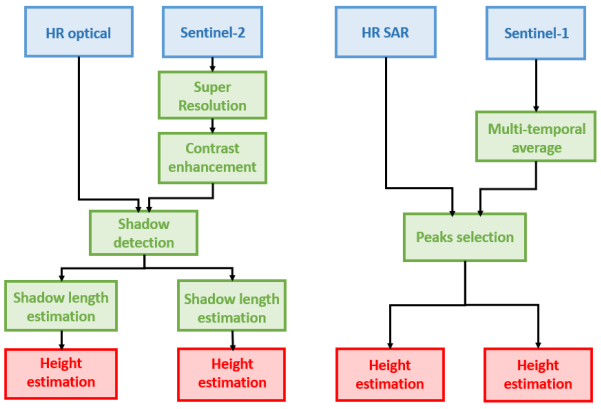

Figure 1: Proposed methods scheme: on the left the optical, on the right the SAR ones. Blue: type of data, Green: algorithms applied, Red: results

2.1. Optical method for tanks height estimation

2.1.1 High resolution method explanation

The optical method which has been presented extracts the height of the tanks from the shadow each of them projects on the ground, exploiting the fact that the shape of the shadow of a tank (both the outer and the inner ones) is a "half-moon" (figure 2).

Figure 2: Example of a tank - optical data

Concerning shadow detection, it has been decided to apply a histogram thresholding technique [2], since it shows the best performance compared to the other state-of-the-art methods [3]. An optimal threshold that maximizes the variance between the classes in the image and automatically divides, in its histogram, the shadows from the rest is found, after inserting a certain number of initial thresholds based on the number of classes present in the image (K classes, K-1 thresholds). A binary shadow mask for each tank is extracted, which is transformed then into a stand-alone polygon. Its convex hull is drawn around it (figure 3a) and its longest segment is selected, that is the distance between the two vertexes of the "half-moon". The midpoint of this segment is calculated and its perpendicular line passing through this point intersects the polygon itself into two other points (A and B in figure 3b), whose distance corresponds to the shadow length measured in pixels.

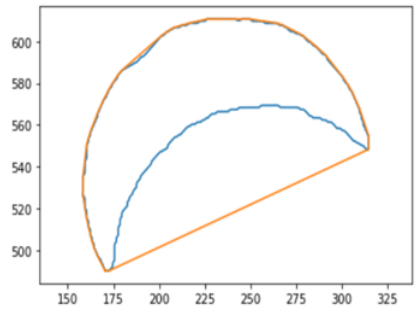

(a) Convex hull

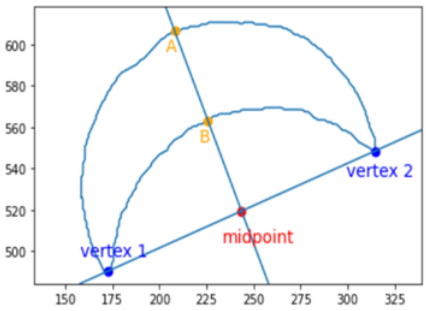

(b) Estimation of shadow length

Figure 3: HR shadow length estimation method. Note: axes values are in pixels

This shadow length (s) is finally converted into the tank height (eq. 1) knowing the Sun incidence angle (θ_{sun}) and the resolution of the image res, that in this case is 0.5m (eq. 2). The actual height has to consider a "look correction" (eq. 3) due to the fact that part of the shadow is covered by the tank itself from the satellite/look point of view (θ_{look}):

$$h = \frac{h_a}{l} \tag{1}$$

where h_a is the "apparent" height and l the look correction, and:

$$h_a = \tan(\theta_{sun}) \cdot \mathrm{s} \cdot \mathrm{res} \tag{2}$$

$$l = 1 - (\tan(\theta_{sun}) \cdot \tan(\theta_{look})) \tag{3}$$

2.1.2 Sentinel-2 method modifications with respect to HR

Sentinel-2 images have a lower resolution (10m), while tanks sizes vary from 20 to 30m of radius and from 12 to 20m of height. Consequently, the shadow shape in Sentinel-2 images is not very

clear because it consists of too few pixels. For this reason, before testing the same method previously mentioned, it was deemed necessary to apply a Super Resolution to the image. The algorithm makes use of Deep Laplacian Pyramid Networks since it has been demonstrated that it is one of the best performing SR algorithms [4]. The HR resolution image is constructed progressively, each time by a factor 2, in a coarse-to-fine fashion. Afterwards, since some shadows were not very visible, it has been decided to apply a contrast enhancement (Contrast Limited Adaptive Histogram Equalization) modifying the lightness component of the image. Despite the super resolution and the contrast enhancement, shadows are not always shaped like a 'half-moon'. Figure 4 shows one of the possible cases in which this occurs.

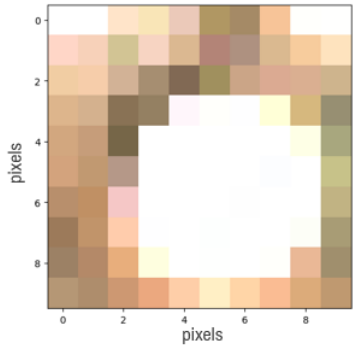

(a) Original Sentinel-2 image

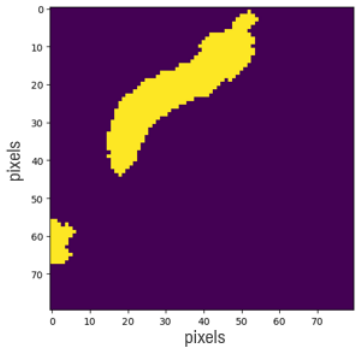

(b) Shadow mask

Figure 4: Example of shadow not shaped like a "half-moon"

It could happen because a part of the shadow of nearby tanks merges with the shadow whose length is being calculated, because of low resolution (few pixels in the scene). However, because of the low resolution itself, it is difficult to state it with certainty. Anyway, the steps that followed in the method used in high resolution, i.e. using the convex hull, can't be applied for Sentinel-2 images and need to be modified. The center on ground of the tank, that is supposed to be known, is used together with the Sun azimuth angle to construct a line crossing the polygon in two points which correspond, as before, to the shadow length (figure 5).

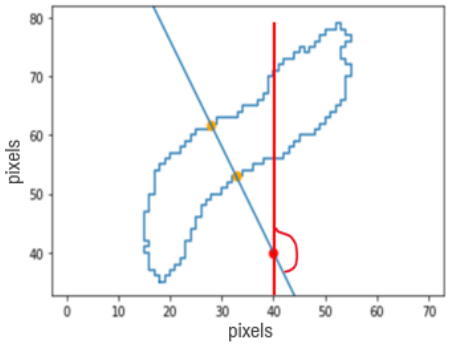

Figure 5: Modification of Sentinel-2 method with respect to HR for shadow length estimation. The red curve indicates the Sun azimuth angle with respect to the North direction

This approach still manages to find the two intersection points with the polygon of interest that correspond to the length of the shadow, considering the direction in which the correct shadow is expected to be, i.e. along Sun azimuth angle. However, it is a limitation with respect to high resolution, since it requires a precise knowledge of the center on ground of the tank, while high resolution approach needs it just to crop the image around a single tank at the beginning of the method.

2.1.3 Application of the optical methods on dataset images

An entire tank terminal is used as dataset (more than 300 tanks).
A result of shadow detection applied to a high resolution optical image on a part of this area is shown in figure 6. As it can be seen, in HR shadows and polygons can be recognized quite well.

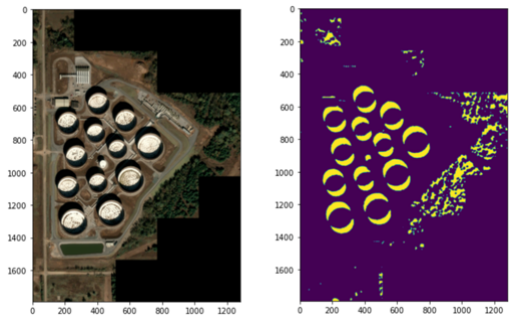

Figure 6: Shadow detection applied to a HR optical image. Note: axes are in pixels for both images

Regarding the parameters used, the number of thresholds in shadow detection algorithm have been set to four, so assuming that the scene is composed by five classes. The assumption comes from the fact that the minimum number of classes in the image is three: the tank itself, its shadow and the background. However, this number has been increased since the background is not homogeneous and it includes different types of terrains and facilities in the surroundings of the tanks (figure 6).
Concerning Sentinel-2 images, the effect of Super Resolution, contrast enhancement and shadow detection on a single tank image can be seen visually in figure 7.

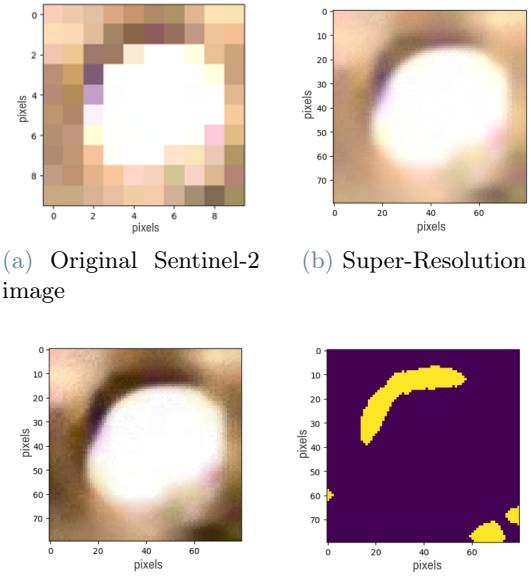

(a) Original Sentinel-2 image (b) Super-Resolution

(c) Contrast enhancement (d) Shadow mask

Figure 7: Sequence of applied algorithms for Sentinel-2 shadow detection

The resulting shadow from the application of Super Resolution is much sharper and similar to the real one with respect to the one in the original image. The resolution achieved is 1.25 meters, since the resolution is 10 meters and the HR factor in SR algorithm is 8. The histograms of the image before and after the contrast enhancement can be seen in figure 8.

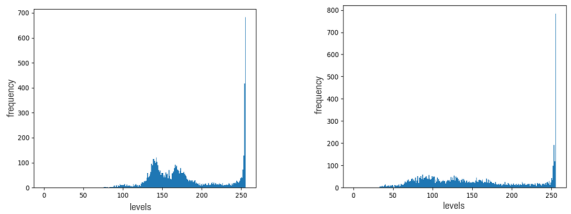

(a) (b)

Figure 8: Histogram before (a) and after (b) the contrast enhancement

256 gray levels are used to represent the image. In the resulting histogram the values are more distributed on the entire range of levels, as it is the purpose of the increase of the contrast.
All numerical results of this sequence are reported in the next section.

2.1.4 Experimental numerical results - Validation of the proposed methods through a comparison with reference data

In order to validate the results, these have been compared to calibrated heights that are considered as reference. First, the mean and and standard deviation of the error (estimated height - reference height) of the preliminary steps applied to the original Sentinel-2, corresponding to the numerical results of figure 7a and 7b, are presented in table 1.

mean	standard deviation
about 1.2 m	about 6 m

(a) initial image, no super resolution, no contrast enhancement

mean	standard deviation
about 45 cm	about 4.6 m

(b) after super resolution, no enhancement

Table 1: Sentinel-2 mean and standard deviation

The final mean and standard deviation, after also contrast enhancement which is the final step before applying the shadow algorithm, is presented with its corresponding histogram of the error distribution (estimated height - reference height) and together with the final results from optical HR (figure 9 and table 2).

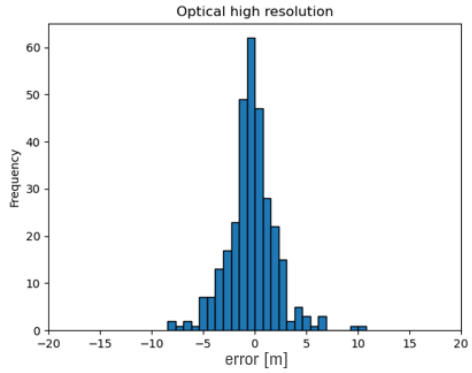

(a) optical HR

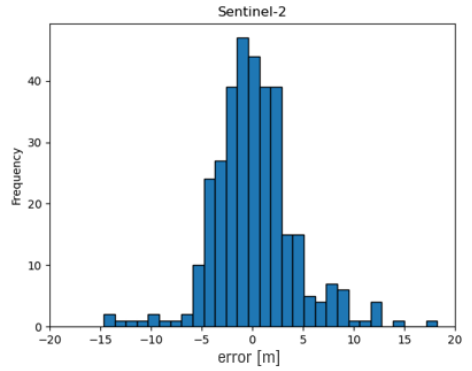

(b) Sentinel-2 (all algorithms applied)

Figure 9: Error distribution

mean	standard deviation
about -30 cm	about 2.4 m

(a) optical HR

mean	standard deviation
about 15 cm	about 4 m

(b) Sentinel-2 (all algorithms applied)

Table 2: Mean and standard deviation

Numerical results show that there was a significant improvement after the entire sequence of Sentinel-2 algorithms.
Since the average height in the tank terminal of interest is 15 meters, the indicative relative error is 16% for HR and 26% for Sentinel-2. Therefore, HR data provide more precise results than Sentinel-2 in terms of standard deviation, as we may expected. However, except for some significant outliers that worsen this parameter with respect to high resolution, the mean in Sentinel-2 image is around zero like high resolution one, meaning that the majority of the estimated heights are similar to the reference data in both cases.
Some "outliers" values emerged from the error distribution because of something unusual in the original image, for example a change in the level of the ground that leads to a deformation of the projected shadow, and consequently the estimated tank height could be very different from the reference one in these particular cases.
The estimated heights in literature regarding the oil tanks were the one of the floating roofs [5], so an accuracy to compare our method with it is not available. In the other articles [3] [2], heights were estimated for buildings, hence parallelepiped-shaped structures. Moreover, the results were compared based on accurate reference shadow masks manually created, and the related accuracy has been calculated as the number of correctly classified pixels with respect to those shadow masks. Since in our proposed method the metric is different, because it has been calculated through a difference between estimated shadow lengths, an exact numerical comparison with existing methods can't be obtained.

2.2. SAR method for tanks height estimation

2.2.1 High resolution method explanation

The presented technique exploits SAR images to find the height of the tanks. Since in a tank SAR image there are mainly three bright peaks (figure 10), the height is estimated through the difference between the leftmost and the center peaks position in range direction, which correspond respectively to the top and the base of the tank (layover), and consequentially to its height in slant range.

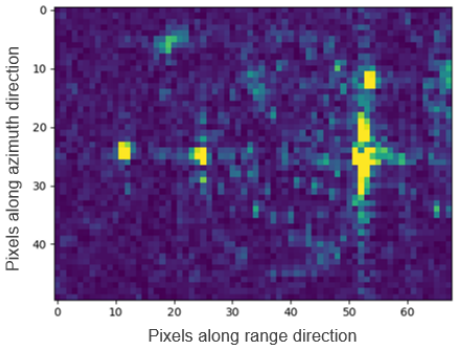

Figure 10: SAR (Iceye) image with the most relevant bright peaks

A geometric model is exploited, because using an electromagnetic one the height could be estimated through the double-reflection bright curve but this requires the knowledge of electromagnetic parameters regarding the ground and the radar itself and they are not known in our case. Therefore the first was preferred.
First, a correct crop of the image is performed transforming the center coordinates of each tank into the acquisition time of the satellite, and the reference radius (r) into its number of pixels in azimuth and in range direction. In azimuth, it is required the satellite velocity (v_s) and the step between pixels (s_{az}), as in eq. 4:

$$r_{az} = \frac{r}{v_s \cdot s_{az}} \tag{4}$$

The same in the range direction, projecting the measure of the radius in slant range (eq. 5 and 5), knowing the incidence angle (θ) and the pixel spacing in range (sp_{rg}):

$$r_{rg} = \frac{r \cdot \sin(\theta)}{sp_{rg}} \tag{5}$$

where:

$$sp_{rg} = \frac{c}{2} \cdot s_{rg} \tag{6}$$

in which c is the speed of light and s_{rg} the range step.
To crop the image in near (with respect to the center) range direction, the measure of the height in slant range is also required. The maximum possible height (in meters) of a tank is retrieved using a database (if this information is not known in general, it can be estimated by a previous general visual inspection), and transformed in pixels in slant range (eq. 7), knowing the incidence angle (θ) and pixel spacing (sp_{rg}):

$$(h_{max})_{[p]} = \frac{(h_{max})_{[m]} \cdot \cos(\theta)}{sp_{rg}} \tag{7}$$

c
A cubic interpolation is then applied in order to select a sub-pixel peaks in the following steps. The profile of the data absolute value [5] along azimuth, summing in the entire range direction, is then calculated and the peak of this profile, that corresponds to the azimuth pixel where the very bright three peaks are, is found exploiting a function that finds the maximum values points with respect to the neighbouring ones (positive left and negative right derivatives). An equal procedure is performed along range, summing in a small window in azimuth direction centered around the azimuth index found in the previous step. The two peaks corresponding to the height will be chosen by the peak function (figure 11).

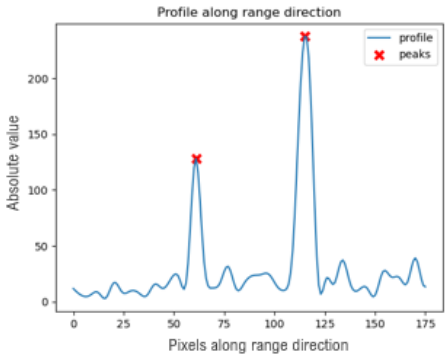

Figure 11: Peaks selection

The height of the tank, in pixels, is calculated through the difference of the range indexes of these two peaks, which is then converted into the actual height (eq. 8), in meters, knowing the range pixel spacing (sp_{rg}) and the incidence angle (θ):

$$h_{[m]} = \frac{h_{[p]} \cdot sp_{rg}}{\cos(\theta)} \tag{8}$$

2.2.2 Sentinel-1 method modifications with respect to HR

The same proposed technique can be applied also on Sentinel-1 images. However, it has been decided to merge more images instead of using just a single one because, as previously mentioned, LR images are more readily available with respect to HR ones and they are also free data. In particular, a multi-temporal average has been calculated, so each pixel value in the final image is the average of each amplitude value along all the images acquired in different times.

2.2.3 Experimental results - Validation of the proposed methods through a comparison with reference data

To assess the accuracy of the proposed method, it is necessary to validate the results comparing the estimated heights with reference heights values, like it has been done for optical images.

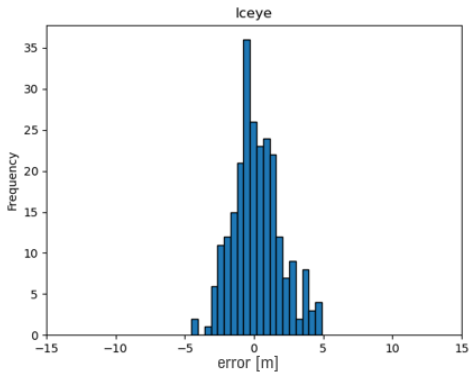

(a) SAR HR

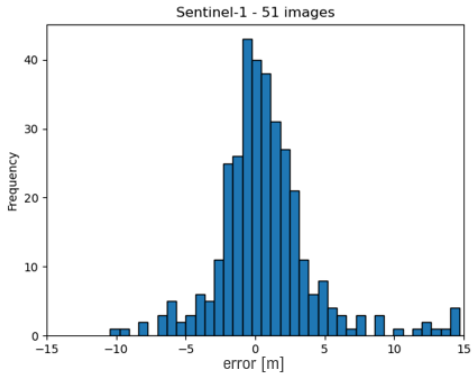

(b) Sentinel-1 (51 images)

Figure 12: Error distribution

mean	standard deviation
about 20 cm	about 1.8 m

(a) SAR HR

mean	standard deviation
about 80 cm	about 3.5 m

(b) Sentinel-1 (51 images)

Table 3: Mean and standard deviation

The error distributions (estimated measure with respect to the reference one) of Iceye and Sentinel-1 is shown above (figure 12), together with their mean and standard deviation (table 3). Since the average height in the tank terminal of interest is 15 meters, the relative error is 12% for Iceye and 23% for Sentinel-1. The standard deviation of SAR HR distribution is halved compared to the one of Sentinel-1. However, except for some significant outliers that worsen the standard deviation with respect to high resolution, the mean in multi-temporal average Sentinel-1 images is around zero like in Iceye one, meaning that the majority of the peaks are correctly identified despite the lower resolution.
Some "outliers" were investigated also in SAR case. For HR these values are due to the fact that in some cases the peaks are not very prominent with respect to the background noise. Concerning Sentinel-1 images, some other bright peaks may appear in the scene in the surroundings of the tank even if an attempt has been made to eliminate them. Hence, the peak function chooses different peaks with respect to the right ones related to the height. In both circumstances, the estimated height can be very different from the reference one.
In literature [6], results have shown an error of about 1 m (estimated - real height), but a mean and a standard deviation have not been specified since the tanks were very few (four). Therefore it is not meaningful to make a comparison with the accuracy of existing methods.

2.2.4 Advantages and disadvantages of multi-temporal average

In order to evince the advantages of multi-temporal average with respect to a single Sentinel-1 image, the mean and standard devi-

ation is calculated for an increasing number of images starting from one (figure 13).

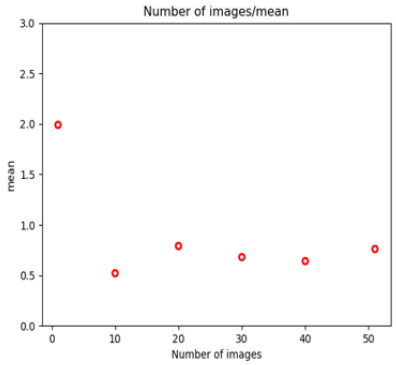

(a)

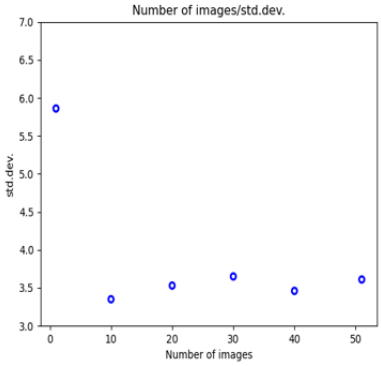

(b)

Figure 13: Number of images and their mean (a) and standard deviation (b)

From 10 to 51 images the two parameters have similar values; however, they are halved comparing them with one single image, proving that using more images improves the accuracy. The reason is that if one or both of the two peaks corresponding to the height, that are supposed to be stable and bright, are instead not very clear in few of them, they can stand out from the background noise anyway and be recognized thanks to multi-temporal average. In addition, the background noise is reduced.
On the other hand, a disadvantage of the multi-temporal average is that if there are high peaks in the surroundings of the tank, even just in a subset of images, the temporal average will have a high value for those pixels in the final image so the algorithm may select wrong peaks in range or azimuth directions.
A slight fluctuation from the values in figure 13 may occur changing which images from the dataset to select in particular.

3. Optical and SAR comparison results - average between estimated heights from the two different sensors

After the analysis and experimental results of the distinct methodologies on optical and SAR images on the same tank terminal, a comparison can be carried out between them. From results in the previous sections, SAR method proved to be more accurate in terms of standard deviation with respect to optical, both for high and low resolution. This is due to the different type of height estimation: because of the different ground levels or glimpses that affect the shadow shape, shadows on ground undergo more significant changes with respect to the ones estimated by SAR, which are simply calculated by the difference between two stable peaks.
Moreover, an average between the height obtained from the two different sensors for each tank is calculated and then compared again with reference data (HR: figure 14 and table 4, Sentinel: figure 15 and table 5).

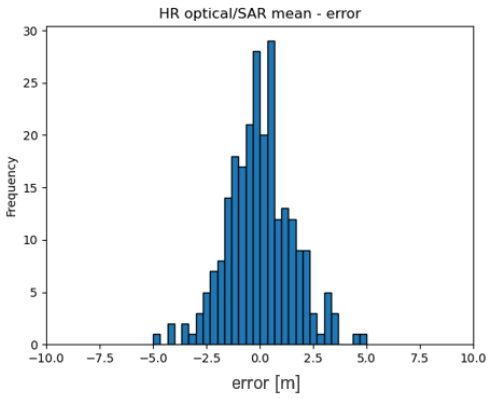

Figure 14: HR optical/SAR average - error

mean	standard deviation
about 0 cm	about 1.5 m

Table 4: HR optical/SAR average - mean and standard deviation

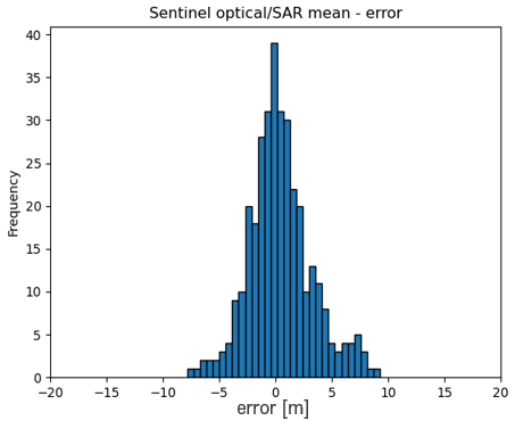

Figure 15: Sentinel optical/SAR average - error

mean	standard deviation
about 45 cm	about 2.8 m

Table 5: Sentinel optical/SAR average - mean and standard deviation

The standard deviation and the total relative error (10% for HR and 18% for Sentinel) are lower than the ones obtained with separate methodologies. This outcome suggests that some estimated heights which are more inaccurate with a sensor are compensated by a more precise measurement obtained from the other one.

4. Conclusions

The objective of this thesis was the estimation of the height of oil tanks exploiting methods based on optical and Synthetic Aperture Radar (SAR). The proposed methods have been explained and analysed both for high and low resolution. Distinct techniques for optical and SAR have been presented: for the first the height has been calculated from the shadow length on ground, while in the latter from the distance between the two bright peaks corresponding to it. The reason behind the choices made in terms of algorithms that have been used were explained. Methodology modifications that are necessary with respect to the HR have been highlighted for Sentinel-1 and Sentinel-2. Experimental results have shown that HR performs better than LR in both cases, as we could expect; however the majority of the tanks have been well recognized also in LR (mean of the error distribution is around zero meters). It has been demonstrated that SAR method is more accurate than optical one in terms of relative error/standard deviation and that averaging the estimates from the two different sensors improves the results in both High and Low resolution. Outliers values have been analysed for possible future developments. The reason why the proposed methods cannot be numerically compared to the existing ones has been explained. Therefore the contribution of the thesis with respect to state-of-the-art methods is to have studied the height of the tanks in more detail, and on an entire terminal, so as to be able to analyze also a distribution of the error and its statistical parameters both for optical and SAR, which had not been done before, and to have also explored the low resolution data, that can be exploited in all those cases in which HR ones are not available or too exclusive.

References

[1] T.A. Gallagher and C.R. Desjardins. *Floating roof tanks - Design and operation in the petroleum industry.* 2000.

[2] R.Doth L.A.Amaral D.F.G. de Azevedo G.F.Silva, G.B.Carneiro. *Near Real-Time Shadow Detection and Removal in Aerial Motion Imagery Application.* 2017.

[3] X. Briottet S.K. Pang N. Paparoditis K.R.M. Adeline, M. Chen. *Shadow detection in very high spatial resolution aerial images: A comparative study.* 2013.

[4] Narendra Ahuja Ming-Hsuan Yang Wei-Sheng Lai, Jia-Bin Huang. *Fast and Accurate Image Super-Resolution with Deep Laplacian Pyramid Networks.* 2019.

[5] Minyoung Back and Taegyun Jeon. *Analysis Of Oil Storage Trend Using KOMPSAT-5 SAR Data.* 2020.

[6] A.Iodice R.Guida and D. Riccio. *Assessment of TerraSAR-X Products with a New Feature Extraction Application: Monitoring of Cylindrical Tanks.* 2010.